Pergamon

J. Geodynamics Vol. 26, No. 2–4, pp. 255–259, 1998

PII: S0264-3707(97)00062-8
0264-3707/98 $19.00+0.00

RESULTS FROM COMBINING TECTONIC OBSERVATIONS AND SAR INTERFEROMETRY FOR THE 1995 GREVENA EARTHQUAKE: A SUMMARY

B. MEYER,[1]* R. ARMIJO,[1] D. MASSONNET,[2]
J. B. DE CHABALIER,[1] C. DELACOURT,[1] J. C. RUEGG,[1]
J. ACHACHE[1] and D. PAPANASTASSIOU[3]

[1]Institut de Physique du Globe, Paris, France
[2]CNES, Toulouse, France
[3]National Observatory, Athens, Greece

(Received 24 January 1997; accepted 13 August 1997)

Abstract—Soon after the 1995 Grevena $M_s = 6.6$ event, we mapped the Palaeochori earthquake fault break. These tectonic observations are combined with the surface displacement field determined with the SAR interferometry to model the fault dislocation at depth.

The 1995 Grevena $M_s = 6.6$ earthquake occurred on May 13, 1995 in north-central Greece, a region with low historical and instrumental seismicity (Papazachos and Papazachos, 1989). After the event several teams conducted field studies including tectonics, geodesy and seismology (Hatzfeld et al., 1995; Pavlides et al., 1995). Here we summarize the main results of a study combining tectonic observations and SAR interferometry (Meyer et al., 1996).

We scrutinized the epicentral region and mapped the earthquake fault break in detail. Although non-tectonic slumps, fissures and landslides were abundant throughout most of the region, unequivocal tectonic rupture was limited to a fairly continuous break along the pre-existing Palaeochori Fault. The Palaeochori Fault is a minor normal fault (topographic relief ≤ 50 m) that strikes N70°E, dips to the NNW and crosses the sediments of the Mesohellenic Trough southeast of Grevena (Fig. 1). The break, which we followed and mapped in detail for 8 km, consisted of open fissures and small scarps with 2–4 cm down-to-the-northwest, normal slip. The surface break is small compared to the moment release of the event (CMT scalar moment of 7.6×10^{18} Nm). At the ENE extremity of the Palaeo-

*Author to whom all correspondence should be addressed: Institut Physique du Globe, Equipe Sismotectonique, 4 place Jussieu, tour 14-15 1er étage, 75252 Paris cedex 05, France; Tel.: 0033 1 44 27 24 29; Fax: 0033 1 44 27 24 40; E-mail: meyer@ipgp.jussieu.fr.

chori Fault, however, numerous small slumps over smaller splaying fault segments indicate that these segments may have also ruptured during the main event. However, we did not find any sign of tectonic rupture east of these faults, across the Vourinos Range, or farther east in the Kozani Basin.

The Palaeochori Fault is part of a larger fault system with similar average strike and dip including the Paliuria and Servia faults, which form a left-stepping en échelon system linked by smaller segments striking N–S to N40°E (Fig. 1). However, the Palaeochori Fault is much smaller than the Paliuria and Servia faults, and the morphological evidence for Quaternary slip is much clearer along the Servia Fault than along the Palaeochori Fault. This evidence suggests that the Servia Fault has average Holocene slip rate in the range of 1–2 mm/yr, and that it is capable of $M \approx 7$ earthquakes every 1000–2000 years (rupture 35 km long, 15 km wide, with 2 m slip per event). Although the morphologic evidence along the Paliuria Fault is less clear, probably because of the different lithology, its slip rate and seismic potential may be comparable. The 1995 earthquake break along the subdued Palaeochori Fault thus reveals reactivation of part of a much larger fault system with interconnecting segments at a range of scales. The system has developed recently (Plio-Quaternary?) across the older Hellenic structure, suggesting that it is in the process of growing.

To explore the 3-D geometrical and mechanical relationships between the different elements of the developing system, we use the surface displacement field determined with the SAR interferometry. We used SAR images of the European satellite ERS-1 (C-band, 56 mm wavelength) to characterize the coseismic displacement field. The images were combined two-by-two using the Digital Elevation Model (DEM) elimination method (e.g., Massonnet et al., 1993) which reveals fringes corresponding to contours of equal change in satellite to ground distance (i.e., range). We produced five interferograms with good coherence spanning periods of 2–3 years and the date of the earthquake. The interferogram selected is the least sensitive to topography (Fig. 1a). It contains mostly coseismic deformation, with eleven main concentric fringes depicting the surface displacement in the ground-satellite line of sight. The fringes are sharp and well-determined on the non-cultivated slopes of the Vourinos Range. Surprisingly, although much more blurred, the fringes are also distinguishable on the plains of the Mesohellenic Trough. That some coherence remains in this area, despite intense agriculture, may be due to stable field borders which survive annual plowing.

The interferogram outlines a 400 km^2 kidney-shaped zone of subsidence reaching 30 cm flanked by an uplift zone reaching 5 cm (Fig. 1a). The southern edge of the subsident area coincides mostly with the break observed along the Palaeochori Fault. However, part of the area of subsidence bypasses the Palaeochori break to the Southeast, toward the splaying NW–SE fault segments. Within this part a set of converging fringes 3 km SE of the eastern extremity of the Palaeochori Fault indicates local scissors faulting. We reproduce the coseismic displacement field using dislocations in an elastic half-space and our observations of the fault system (Fig. 1b,c). We proceeded by trial and error integrating the tectonic constraints and increasing progressively the complexity of the model to fit quantitatively the details of the SAR information. The problem has no unique solution, and we show here one reasonable model explaining the main features of the coseismic faulting (Fig. 1c). However, by using a range of information we increase the probability that it is close to reality. We note that inversion techniques could be used but less easily incorporate widely differing data sets.

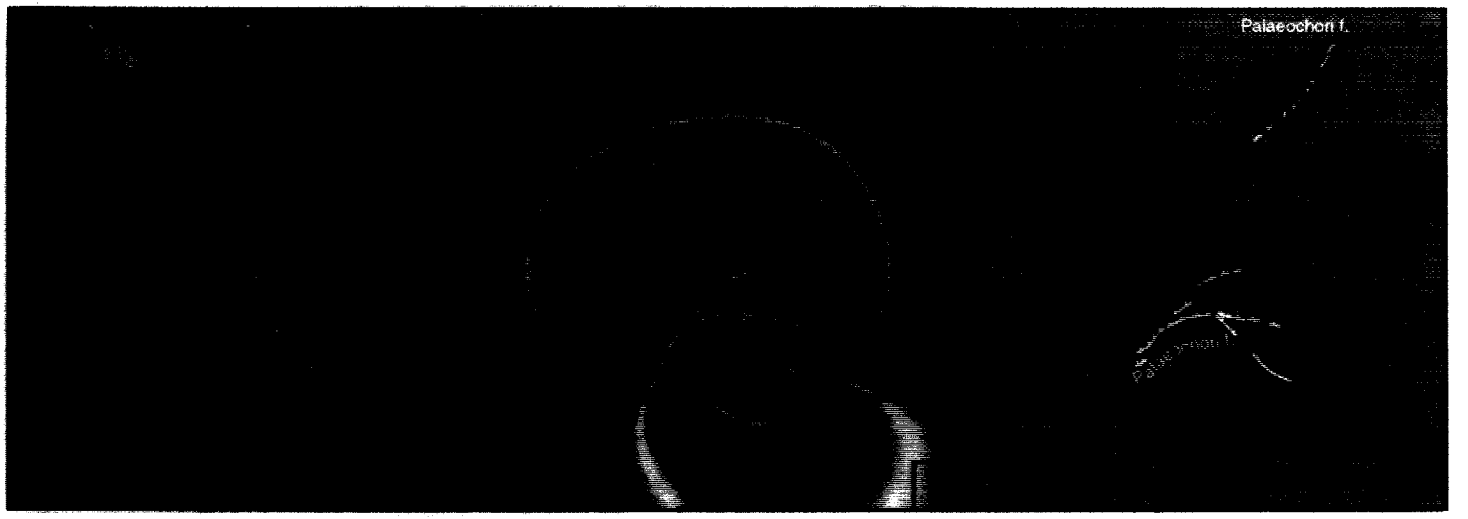

Fig. 1. Modelling of combined SAR and tectonic observations. The 1995 Grevena earthquake ($M_s = 6.6$) ruptured the Palaeochori Fault and the smaller splays at its eastern extremity (white), but not the larger Paliuria and Servia Faults (black). (**a**) Interferogram describing the surface displacement between 16/11/93 and 05/10/95, with an altitude of ambiguity of 126 m and an error of less than 2 mm. Each fringe represents 28 mm of displacement. Unit vector from the ground to the satellite [east, north, up] is [0.402, −0.083, 0.912]. (**b**) Synthetic fringes from the elastic dislocation modelling. (**c**) Corresponding fault model with the average displacement (in m). The two patches with 0.4 m have variable slip, see text. Inset section: Modelled Palaeochori fault and surface vertical displacement (in cm, segmented). Main shock with error bars and aftershocks (over 14 km wide band) are from Hatzfeld et al. (1995).

The fringe pattern can be fit with normal faulting on rectangular planes intersecting the surface at the traces of the mapped faults (Fig. 1c). The western half of the subsidence area requires that the Palaeochori Fault has a steeper dip near the surface than at depth. We take 60° dip from the surface to 9 km depth, and a dip of 40° down to 15 km. Average slip is 1 m at depth, but it has to decrease rapidly to 5 cm within the 4 km near the surface. The eastern part of the subsidence area requires rupture of the two ENE-dipping faults southeast of the Palaeochori Fault. For the southern splay, which parallels the structure of the Vourinos, we take dip of 60° and average slip of 0.3 m within a patch not reaching the surface, from 2 to 10 km depth. For the nearly E–W splay (immediately east of the Palaeochori Fault) we take the same dip but reaching to the surface with slip that tapers from 0.6 m to 0.1 m to the ESE, in agreement with the scissors faulting seen in the interferogram. Finally, average slip of 0.3 m is needed for the en echelon splays parallel to the Palaeochori Fault (NE of it), to reproduce the centre of maximum subsidence in the interferogram.

The model explains well the kidney shape of the hangingwall fringes, their number and the local gradients. It also reproduces satisfactorily the bulge in the footwall. The small break observed along the Palaeochori Fault is the surface expression of larger slip on the same structure at depth. However, to fit in detail the complexities in the best defined part of the fringes requires slip reaching the surface on the minor fault segments where the surface break in the field was less certain, NE and SE of the Palaeochori Fault. In any case the eastern part of the 1995 rupture appears to splay into several segments as it enters the Vourinos Range. This implies scissors faulting and probably reactivation, under extension, of a patch of an old Hellenic thrust plane with NW–SE strike and NE dip. The 1995 rupture along the Palaeochori Fault mimics the bend in the geometry of the Paliuria Fault farther south. This suggests that the former is possibly encountering the same mechanical obstacles as the latter as it propagates across the Vourinos structure. This geometry implies some amount of stretching directed NE–SW. A full account of the details of the kinematics and of the mechanical implications is out of the scope of this summary paper and will be given elsewhere.

Our preliminary model is not inconsistent with the mainshock hypocenter and with the aftershock distribution. Taking shear modulus of 33 GPa, the model yields total seismic moment of 6.4×10^{18} Nm, nearly the same as the CMT. About 80% of the total moment is released by slip on the Palaeochori Fault and 45% on its 40° dipping part, in agreement with the long-period fault plane solution. The secondary splay faulting at the NE extremity of the Palaeochori Fault is well resolved and release no more than 20% of the total moment. No other source of complexity (e.g., secondary antithetic faulting) is required at this stage. Further work is needed to resolve better the model with additional tectonic and seismological constraints.

Acknowledgements—This work was funded by the French INSU-CNRS (PNRN) and EC (Environment and Climate) Programs. IPGP contribution No 1507.

REFERENCES

Hatzfeld, D., Nord, J., Paul, A., Guiguet, R., Briole, P., Ruegg, J-C., Cattin, R., Armijo, R., Meyer, B., Hubert, A., Bernard, P., Macropoulos, K., Karakostas, V., Papaioannou, C., Papanastassiou, D. and Veis, G. (1995) The Kozani–Grevena (Greece) earthquake of

May 13, 1995, Ms = 6.6, Preliminary results of a field multidisciplinary survey. *Seismological Research Letters* **66**(6), 61–70.

Massonnet, D., Rossi, M., Carmona, C., Adragna, F., Peltzer, G., Feigl, K. and Rabaute, T. (1993) The displacement field of the Landers earthquake mapped by radar interferometry. *Nature* **364**, 138–142.

Meyer, B., Armijo, R., Massonnet, D., de Chabalier, J. B., Delacourt, C., Ruegg, J. C., Achache, J., Briole, P. and Papanastassiou, D. (1996) The 1995 Grevena (Northern Greece) earthquake: fault model constrained with tectonic observations and SAR interferometry. *Geophys. Res. Letter* **23**(19), 2677–2680.

Papazachos, B. C. & Papazachos, C. B. (1989) *The earthquakes of Greece*, (in Greek), pp. 356. Ziti Publications, Thessaloniki.

Pavlides, S., Zouros, N., Chatzipetros, A., Kostopoulos, D. and Mountrakis, D. (1995) The 13 May 1995 western Macedonia, Greece (Kozani Grevena) earthquake; preliminary results. *Terra Nova* **7**, 544–549.